Mitochondrial origin-binding protein UMSBP mediates DNA replication and segregation in trypanosomes

Neta Milman*, Shawn A. Motyka†, Paul T. Englund†, Derrick Robinson‡, and Joseph Shlomai*§

*Department of Parasitology, The Kuvin Center for the Study of Infectious and Tropical Diseases, Hebrew University–Hadassah Medical School, Jerusalem 91120, Israel; †Department of Biological Chemistry, Johns Hopkins University School of Medicine, Baltimore, MD 21205; and ‡Microbiologie Cellulaire et Moléculaire et Pathogénicité (MCMP) Unité Mixte de Recherche–Centre National de la Recherche Scientifique 5234, Université Bordeaux 2, 146 Rue Léo Saignat, Bât. 3A, 33076 Bordeaux CEDEX, France

Edited by I. Robert Lehman, Stanford University School of Medicine, Stanford, CA, and approved October 19, 2007 (received for review July 22, 2007)

Kinetoplast DNA (kDNA) is the remarkable mitochondrial genome of trypanosomatids. Its major components are several thousands of topologically linked DNA minicircles, whose replication origins are bound by the universal minicircle sequence-binding protein (UMSBP). The cellular function of UMSBP has been studied in *Trypanosoma brucei* by using RNAi analysis. Silencing of the trypanosomal *UMSBP* genes resulted in remarkable effects on the trypanosome cell cycle. It significantly inhibited the initiation of minicircle replication, blocked nuclear DNA division, and impaired the segregation of the kDNA network and the flagellar basal body, resulting in growth arrest. These observations, revealing the function of UMSBP in kDNA replication initiation and segregation as well as in mitochondrial and nuclear division, imply a potential role for UMSBP in linking kDNA replication and segregation to the nuclear S-phase control during the trypanosome cell cycle.

kDNA replication initiation | kDNA segregation | kinetoplast DNA | trypanosomes cell cycle control | universal minicircle sequence-binding protein

Kinetoplast DNA (kDNA) is a unique extrachromosomal DNA, found in the single mitochondrion of trypanosomatids. It consists, in the different species, of a few dozen maxicircles (20–40 kb each) and a few thousand minicircles (0.5–10 kb each), that are interlocked topologically into a DNA network (1, 2). Minicircles in most trypanosomatid species contain two short sequences that are associated with replication initiation: a dodecamer, designated the universal minicircle sequence (UMS), and a hexamer. These sequences have been mapped to the replication origins of the minicircle's light (L) and heavy (H) strands, respectively.

kDNA replication occurs during S phase of the cell cycle, approximately in parallel with nuclear DNA replication (3). Minicircles are released from the network into the kinetoflagellar zone, located in the mitochondrial matrix, between the kDNA network and the flagellar basal body. Each minicircle replicates as an individual replicon, forming gapped and nicked progeny molecules. Minicircle replication intermediates then migrate onto two antipodal sites, flanking the kDNA disk, in which primer-removal, repair of the gaps between Okazaki fragments and reattachment of the progeny minicircles to the network occurs. The final gap-filling and sealing of the topologically linked minicircles take place before the network division (recently reviewed in refs. 1 and 2).

We have previously reported the presence in *Crithidia fasciculata* of a UMS-binding protein (UMSBP). The protein, which contains five tandemly arranged CCHC-type zinc-finger motifs, has been purified from cell extracts, and its encoding gene and genomic locus were cloned and analyzed (4–7). Genes encoding orthologous proteins have been identified in other trypanosomatid species [ref. 8 and supporting information (SI) Table 1]. UMSBP binds specifically the two conserved sequences, located at the minicircle replication origins: the UMS dodecamer and an H-strand 14-mer sequence, containing the conserved hexamer (4, 9). Immunolocalization of UMSBP in *C. fasciculata* revealed two distinct protein foci in the kinetoflagellar zone, near the suggested site where minicircle replication initiates (10, 11). On the basis of its recognition of conserved origin sequences, its intramitochondrial localization and its presence in the kinetoplast during S phase (10), it has been proposed that UMSBP functions as an origin-binding protein, which triggers replication initiation and recruits other replication proteins to this site.

Here, we have studied the function of UMSBP in the trypanosomatid cell cycle, using RNAi, to silence the two *UMSBP* genes encoding UMSBP orthologues in *Trypanosoma brucei*. Our observations support a function for UMSBP as a minicircle replication-initiator protein and revealed yet other, postreplication functions of UMSBP during kDNA segregation, nuclear mitosis, and the cell cycle proceeding. The results suggest that UMSBP may play a role in linking kDNA replication and segregation to the nuclear S-phase control.

Results

***T. brucei* Genome Contains Two UMSBP Orthologues.** The *T. brucei* genome contains two genes with high resemblance to *cfUMSBP* (SI Fig. 6). One gene (Tb10.70.0800), designated *tbUMSBP1*, encodes a predicted 140-aa protein, which, like the *C. fasciculata* UMSBP, contains five CCHC-type zinc fingers. The second (Tb10.70.0820), designated *tbUMSBP2*, encodes a predicted 213-aa protein, containing seven predicted CCHC-type zinc fingers. The predicted tbUMSBP1 and tbUMSBP2 proteins share 52% identity between them and 50% and 51% identity, respectively, with cfUMSBP.

We used EMSA analysis of *T. brucei* cell extracts to assay for proteins that bind a UMS single-stranded oligonucleotide ligand. Two nucleoprotein complexes were identified (SI Fig. 7*A*). Based on the predicted molecular masses of the *T. brucei* putative UMSBP proteins and the RNAi analyses described below (Fig. 1 and SI Fig. 8), the higher-electrophoretic mobility band represents nucleoprotein complex with tbUMSBP1, whereas the lower-mobility band has resulted from UMS interaction with tbUMSBP2. Polyclonal antibodies raised in rabbits against *C. fasciculata* UMSBP, which cross react with *T. brucei* UMSBPs, were used in Western blot analyses of *T. brucei* cell extracts. The identification in these analyses (SI Fig. 7*B*) of two protein bands with the apparent masses predicted from the *tbUMSBP1* and *tbUMSBP2* ORFs, confirms the expression of tbUMSBP1 and tbUMSBP2 proteins in *T. brucei*.

Immunofluorescence analysis shows (Fig. 1*A*) that similarly to

Author contributions: N.M. and J.S. designed research; S.A.M. and P.T.E. contributed new reagents/analytic tools; N.M. and D.R. performed research; N.M., S.A.M., P.T.E., D.R., and J.S. analyzed data; and N.M., P.T.E., D.R.R., and J.S. wrote the paper.

The authors declare no conflict of interest.

This article is a PNAS Direct Submission.

§To whom correspondence should be addressed. E-mail: josephs@ekmd.huji.ac.il.

This article contains supporting information online at www.pnas.org/cgi/content/full/0706858104/DC1.

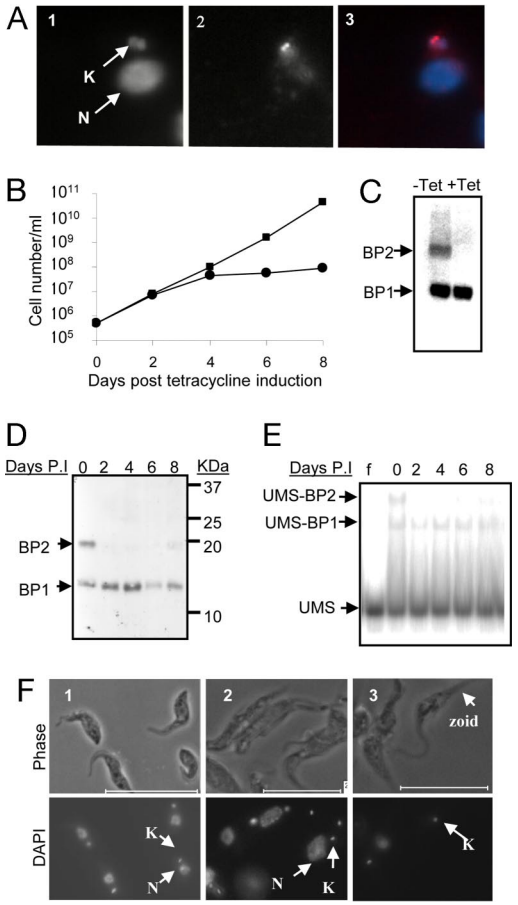

Fig. 1. Silencing the *tbUMSBP2* gene in *T. brucei* affects nuclear mitosis. (*A*) Intramitochondrial immunolocalization of UMSBP. (1) DAPI staining of the *T. brucei* nucleus (N) and the kinetoplast disk (K); (2) immunostaining using anti-UMSBP antibodies; and (3) merging of the latter images. Immunofluorescence of the uninduced cells was as described in *Materials and Methods*. (*B–F*) Cell cultures harbor the pZJMBP2 plasmid. (*B*) Growth curves of cloned cells with (circles) and without (squares) tetracycline induction. (*C*) Northern blot hybridization analyses of RNA, extracted from uninduced (−TET) or RNAi-induced cells (+TET) 48 h after addition of tetracycline. The probe also recognizes *tbUMSBP1* gene (lower band) because of the high homology between the sequences. (*D*) Western blot analysis of whole-cell lysates from uninduced cells (day 0) and in samples withdrawn from induced cells, at the indicated time intervals after RNAi induction (P.I) (days 2–8). (*C* and *D*) BP1 and BP2 denote tbUMSBP1 and tbUMSBP2 mRNA and protein, respectively. (*E*) EMSA analysis of extracts prepared from *T. brucei*-induced cells by using a UMS ligand. One microgram of protein of cell extracts, prepared from cells before tetracycline induction (day 0) and from cell samples withdrawn at the time intervals indicated after induction (days 2–8); lane f, free UMS, no protein was added. (*F*) Phase-contrast and DAPI fluorescence microscopy of images of *T. brucei* cells during *tbUMSBP2* RNAi induction. (1) Images of uninduced *T. brucei* cells. (2 and 3) Cells with large nuclei and a zoid cell, respectively, from day 6 after *tbUMSBP2* RNAi. (Scale bars: 15 μm.)

its localization in *C. fasciculata* (9), *T. brucei* UMSBP resides within the kinetoplast at two discrete foci located near the kDNA disk. We cannot distinguish the relative contribution of tbUMSBP1 and tbUMSBP2 to this signal, but such mitochondrial localization was also detected in cells in which either *tbUMSBP1* or *tbUMSBP2* genes were knocked down (N.M. and J.S., unpublished data). Significantly, no signal could be detected under these conditions in the cell nuclei.

RNAi Silencing of the *tbUMSBP* Genes. To study the function of UMSBP1 and UMSBP2, we used a tetracycline-inducible RNAi system (12, 13). Northern blot analyses revealed a nearly complete loss of *tbUMSBP1* and *tbUMSBP2* mRNAs within 48 h after RNAi induction (SI Fig. 8*B* and 1*C*). RNAi of *TbUMSBP1* had no effect on cell growth (SI Fig. 8*A*). However, RNAi of *tbUMSBP2* caused a significant growth inhibition, with a complete cessation of cell division between days 4 and 8 after RNAi induction (Fig. 1*B*). Resumption of cell growth after this period was most probably due to the presence of revertant cells (14).

The level of *tb*UMSBP1 and *tb*UMSBP2 was monitored by Western blot analyses (SI Fig. 8*C* and Fig. 1*D*). As shown in SI Fig. 7*B*, the antibodies recognize two protein bands in *T. brucei* cell extracts. RNAi of *tbUMSBP1* caused the loss of the majority of lower *tb*UMSBP1 band with no significant effect on the upper *tb*UMSBP2 band. Silencing of the *tbUMSBP2* gene resulted in the complete depletion of the upper protein band with no detectable change in the *tb*UMSBP1 protein band.

We next investigated whether RNAi of the *tbUMSBP* genes influences the UMS-binding activity detected in cell extracts. SI Fig. 8*D* and Fig. 1*E* show EMSA assays, which monitor the effect of RNAi on UMS-binding activity for *tbUMSBP1* and *tbUMSBP2*, respectively. RNAi of *tbUMSBP1* (SI Fig. 8*D*) resulted in the loss of the faster migrating nucleoprotein complex, confirming that this complex contains tbUMSBP1. Silencing *tbUMSBP2* results in the disappearance of the upper nucleoprotein complex, confirming that it has, indeed, been generated by the interaction of tbUMSBP2 protein and UMS DNA, because the complex displaying a higher-electrophoretic mobility is little affected. An increase in intensity of the nucleoprotein complex generated by tbUMSBP2 was observed in *tbUMSBP1* RNAi-induced cells (SI Fig. 8*D*).

Silencing of *tb*UMSBP2 Affects Nuclear Mitosis. We monitored morphological changes in the nuclei and kinetoplasts as a result of RNAi induction, using phase and fluorescence microscopy. These analyses revealed that, whereas the silencing by RNAi of *tbUMSBP1* resulted in no detectable morphological changes (SI Fig. 8*E*), RNAi of *tbUMSBP2* resulted in significant changes in the cells dimensions (compare Fig. 1*F*1 to 1*F*2 and 1*F*3). *tbUMSBP2*-silenced cells show the presence of significantly enlarged nuclei (Fig. 1*F*2). Our measurements revealed a variable, but significant, increase of up to 2-fold in the area occupied by nuclei and their mean fluorescence intensity in RNAi induced cells, as compared with the uninduced cells. Significantly, induced cells display increased abundance (of 15%, compared with 2% in uninduced cultures) of cells containing one kinetoplast and no nucleus (1K0N) (Fig. 1*F*3). This type of cell, known as zoid, is generated by cytokinesis of cells that have replicated their kDNA in the absence of nuclear DNA replication and/or mitosis. The zoid's sister cell is 1K1N (15). It appears that silencing of *tbUMSBP2* resulted in inhibition of nuclear mitosis, because their nuclear area indicates that the DNA was already doubled, but its segregation has been impaired.

Simultaneous Silencing of the Two *tbUMSBP* Genes Results in Earlier Growth Arrest. Silencing of the *tbUMSBP1* gene has no detectable effect on either kDNA replication (N.M. and J.S., unpublished data) or the cell growth rate (SI Fig. 8*A*). A possible explanation could be that the two UMSBPs are functionally redundant, allowing tbUMSBP2 to substitute for tbUMSBP1. To address this possibility, we have induced RNAi with a pZJM construct, which contains fragments of both *tbUMSBP* genes. As shown in Fig. 2*A*, the growth rate of the induced culture decreases after 2 days of RNAi, and cell growth stops completely by day 4. Northern blot analysis of RNA prepared from uninduced cells and from cells after 2 days of RNAi, indicates a dramatic decrease in the mRNA levels of both *tbUMSBP* genes and appearance of RNA degradation products (Fig. 2*B*). Western blot analysis shows that the levels of both proteins decrease to

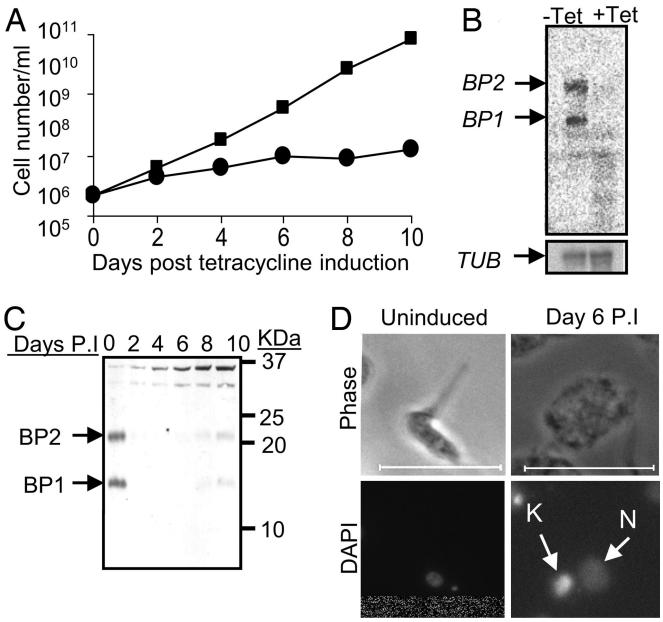

Fig. 2. The simultaneous silencing of *tbUMSBP1* and *-2* generates cells with enlarged nuclei and unsegregated kDNA networks. Cell cultures harbor the pZJMBP1 and -2 construct (expressing simultaneously *tbUMSBP1* and *tbUMSBP2* sequences). (*A*) Growth curves of cells with (circles) and without (squares) tetracycline induction. (*B*) Northern blot hybridization analyses of RNA, extracted from uninduced cells (−Tet) and RNAi-induced cells 48 h after addition of tetracycline (+Tet). The membrane was also probed with *TUBULIN* (*TUB*) probe as a loading control. (*C*) Western blot analysis of whole-cell lysates; uninduced and of samples withdrawn from induced cells after RNAi induction (P.I) at the indicated time intervals. BP1 and BP2 denote tbUMSBP1 and tbUMSBP2 mRNA and protein, respectively. (*D*) Phase-contrast microscopy and fluorescence microscopy of DAPI-stained *T. brucei* cells before and after 6 days of *tbUMSBP1* and *-2* RNAi. (Scale bars: 15 μm.)

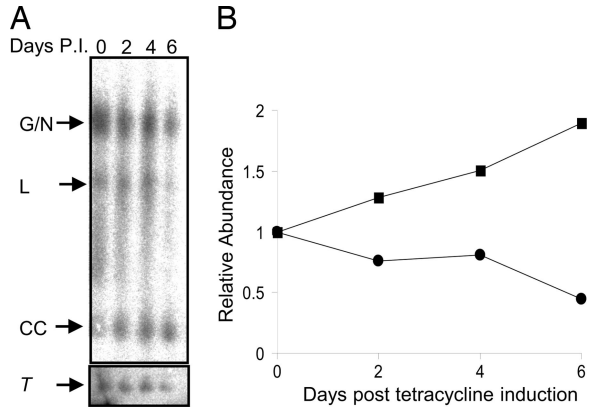

Fig. 3. Silencing of *tbUMSBP1* and *-2* results in the inhibition of minicircle replication initiation. (*A*) Whole DNA was prepared from cell samples, withdrawn at the indicated time intervals after simultaneous *tbUMSBP1* and *tbUMSBP2* RNAi induction. Three hundred nanograms of DNA was electrophoresed in a 1.5% agarose gel, in the presence of 1 μg/ml ethidium bromide, and transferred onto a nitrocellulose membrane. kDNA was detected by using a ^{32}P-labeled minicircle probe. DNA from uninduced cells (day 0) and at the indicated time intervals after RNAi induction (P.I) were analyzed. Arrows indicate gapped and nicked (G/N), linear (L), and covalently closed (CC) minicircles. Levels of nuclear DNA during UMSBPs RNAi were determined by reprobing the same blot for *TUBULIN* (*T*). (*B*) Quantification of the PhosphorImager images in *A*, demonstrating the relative abundance of covalently closed (squares) and gapped and nicked (circles) free minicircles. Values represent the abundance of each minicircle form, relative to its abundance in the uninduced cells. To correct for unequal loading of the lanes the amount of minicircle DNA was normalized to nuclear DNA.

undetectable levels by day 2 of RNAi (Fig. 2*C*). The source of the slow migrating bands, which are probably the result of a cross reaction with the polyclonal anti-UMSBP antibodies, is as yet unknown.

Silencing of both *tbUMSBP* Genes Inhibits Minicircle Replication Initiation. RNAi silencing of either of the individual *tbUMSBP* genes has revealed neither significant change in the size of kinetoplasts (Fig. 1*F* and SI Fig. 8*E*) nor in the abundance of minicircle replication intermediates (N.M. and J.S., unpublished data). Therefore, we have silenced simultaneously *tbUMSBP1* and *tbUMSBP2* to determine the effect on the free minicircle replication intermediates. Minicircle replication starts with the prereplication release of covalently closed minicircles from the network into the kinetoflagelar zone, where replication occurs, generating nicked and gapped replication intermediates. Fig. 3 shows a Southern blot hybridization analysis of an agarose–ethidium bromide gel, which resolves prereplicated, covalently closed (CC) free minicircles and gapped and nicked (G/N) replication intermediates. These analyses revealed an increase of ≈2-fold in the covalently closed free minicircles, with a concomitant decrease (of 2-fold) in the gapped and nicked replication intermediates in the induced cells, after 6 days of RNAi, over the uninduced cells (time 0). A low background of linearized minicircles, which are not minicircle replication intermediates, could also be detected upon long exposure of the membrane. Their quantification reveals a constant low level during RNAi. The increase in abundance of free prereplicated covalently closed minicircles and the decrease in generation of gapped and nicked replication intermediates as the result of *tbUMSBPs* RNAi suggest that covalently closed minicircles are released from the kDNA network but fail to initiate efficiently their replication, implying a role for UMSBP in this process.

Silencing of the *tbUMSBP* Genes Affects Cell Ploidy and Morphology. Phase-contrast microscopy analyses of *tbUMSBPs* RNAi-induced cells have revealed that approximately half of the cells have an unusual morphology, displaying a more rounded and less slender shape. Moreover, fluorescence microscopy revealed, remarkably (Fig. 2*D*), that after 6 days of RNAi, ≈70% of the cells contained significantly enlarged kinetoplast and nucleus, with both organelles displaying a significantly higher fluorescence intensity in comparisons with these organelles in the uninduced cells. These observations may indicate either an increase in their DNA content or in the accessibility of the stain due to a change in the organization of kDNA, or both. These results indicated that DNA segregation in both organelles may have been impaired. In accord with this notion are FACS analyses of the same RNAi cell line, stained with propidium iodide, which indicate that knockdown of the two *tbUMSBP* genes resulted in a decrease in abundance of G_1 cells in the population (from 42 to 29%) and a significant (>3-fold) increase in the abundance of cells whose DNA content is higher than in G_2 cells (Fig. 4*B*).

Simultaneous RNAi of *tbUMSBPs* Causes Accumulation of Giant kDNA Networks. To further characterize the large kinetoplasts, we isolated kDNA networks, from RNAi-induced and uninduced cells and purified the isolated networks using sucrose gradients, stained them with DAPI, and monitored their size (Fig. 4*A*). By day 6 of the RNAi, we observed, as expected, larger and more intensively fluorescing networks, as compared with those found in uninduced cultures. Measurements of the mean area occupied by each of 200 isolated kDNA networks showed large variation of these values among the isolated networks, with a significant

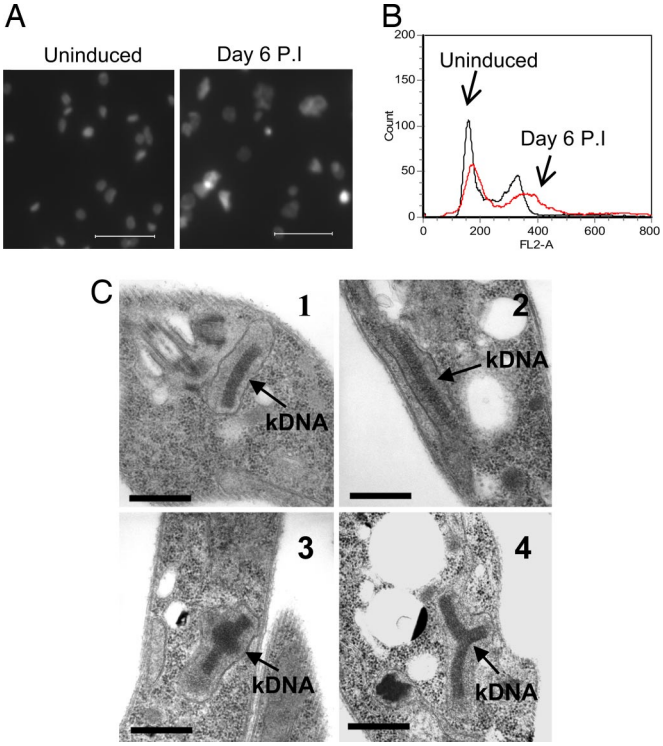

Fig. 4. Silencing for *tbUMSBP1* and *-2* impairs the segregation of kDNA networks. (*A*) kDNA networks, purified by using sucrose gradients, were DAPI-stained and visualized by fluorescence microscopy before and on day 6 of RNAi induction (P.I). (*B*) FACS analysis of uninduced cells (black line) and cells from day 6 after induction (red line) of *tbUMSBP1* and *-2* RNAi, performed as described (34). (*C*) Thin sections of uninduced cells (1) and cells at day 6 (2–4) after the RNAi induction were analyzed by electron microscopy. Minicircles are reattached to the replicating kinetoplast (black arrow) in an abnormal manner whereby the network either increases in diameter (2) or on both faces of the replicating disk (3). Perturbation in the network results in disruption of segregation and, ultimately, segregation blockage (4). (Scale bars: *A*, 15 μm and *C*, 0.5 μm.)

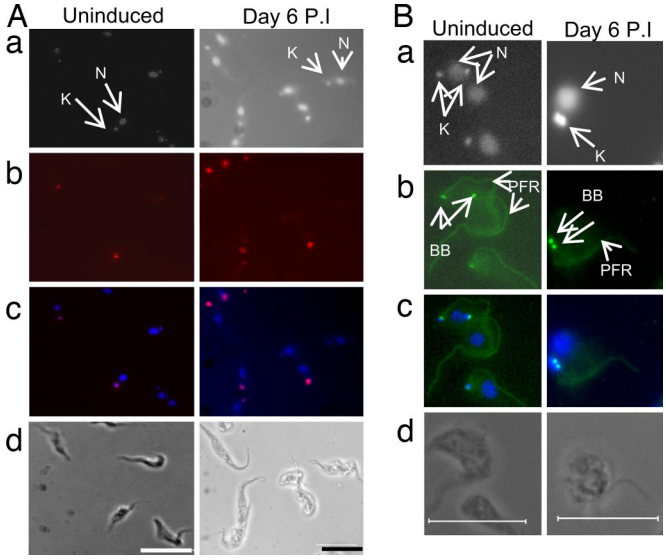

Fig. 5. Silencing of *tbUMSBP* genes yields gapped unsegregated networks and impedes the separation of the flagellar basal bodies. (*A*) Uninduced cells (*Left*) and cells at day 6 after *tbUMSBP1* and *-2* RNAi induction (*Right*) were fixed, stained with DAPI (*a*), and submitted to a gap-filling reaction *in situ* by using terminal deoxynucleotidyl transferase and fluorescent dUTP (35) (*b*). (*c*) A merge of the images in *a* and *b* is shown and (*d*) phase-contrast microscopy is shown. (*B*) Uninduced *T. brucei* cells (*Left*), and cells after 6 days of *tbUMSBP1* and *-2* RNAi induction (*Right*) were fixed, permeabilized, stained with DAPI (*a*), and immunostained by using the basal body antibody BBA4 and an axoneme protein antibody Mab25 (*b*). (*c*) A merge of *a* and *b* is shown. (*d*) Phase-contrast microscopy is shown. (Scale bars: 15 μm.)

increase in the average surface area of isolated kDNA networks during RNAi (Fig. 4*A*) as compared with uninduced cells. Although no measurable change could be detected in the mean area occupied by the isolated networks at day 2 after RNAi induction as compared with the value measured in uninduced cells, this value increases significantly during day 4 (≈2-fold) and day 6 (≈3-fold) of RNAi.

Examination of thin sections of the induced and uninduced cells by electron microscopy revealed that the ultrastructure of kDNA networks in the RNAi-induced cells displays some peculiar features. Some of these networks were apparently condensed into disks, similar to those in uninduced cells, but with larger diameter (Fig. 4*C*, compare 1 and 2). Other networks in induced cells looked as though they had apparently disorganized kDNA accumulated at both faces of the disk (Fig. 4*C*3). Still other networks seem to be interrupted during the process of kDNA network segregation (Fig. 4*C*4). We suggest that these densely packed networks have resulted from the addition of replicated minicircles that have escaped the inhibition of replication initiation (Fig. 3), and accumulated due to lack of network segregation, but also incorrect network organization.

Unsegregated Networks in *tbUMSBPs*-Silenced Cells Contain Gapped DNA Minicircles. To study the status of gap-filling of minicircles in the giant kDNA networks, we have used the *in situ* incorporation of fluorescently labeled dUTP into kDNA networks by terminal deoxynucleotidyl transferase (TdT) (16). Under normal growth conditions, the final gap filling and sealing of replicated minicircles occurs after their reattachment to the kDNA network, possibly through the action of DNA polymerase β-PAK and ligase kα (17–19). Indeed, in uninduced cells, most of the kDNA networks were of an apparently normal size and were negative for the dUTP fluorescence signal, whereas larger kDNA networks display a fluorescence signal, indicating that they were replicating networks containing gapped minicircles (Fig. 5*A*). When ≈100 RNAi-induced and -uninduced cells were screened for fluorescence labeling, following *in situ* labeling, an increase of 50% in positive cells was observed at day 6, in the cells induced simultaneously for the *tbUMSBPs* RNAi, relative to uninduced cells. Most of the networks in the induced cells were of significantly larger size and incorporated more extensively the fluorescent nucleotide, indicating their high content of gapped DNA minicircles.

Flagellar Basal Bodies Segregation Is Impaired in *tbUMSBP1* and *-2* Knocked-Down Cells. The basal body and the kinetoplast in trypanosomatids are linked through a filament system (20, 21). Moreover, it has been observed that the kinetoplast segregation process is mediated by the separation of the basal bodies (21). To examine whether basal bodies are correctly separated in cells silenced for the *tbUMSBP* genes, we have used immunofluorescence, using the monoclonal antibody BBA4 (22). Other studies reporting defects in kDNA replication have shown that, even though kDNA was not replicated the network was separated, albeit asymmetrically, due to basal body movement (1, 23). Here, however, in the *tbUMSBPs*-silenced cells, we observe the impairment of basal bodies segregation (Fig. 5*B*). Large kDNA networks with two basal bodies were observed, in which separation of the two basal bodies had started, but was not completed. Immunostaining of the paraflagellar rod (PFR) (Fig. 5*B*)

reveals that RNAi silencing of the *UMSBP* genes impairs the process of separation of the two flagella. Whereas in the uninduced cells, both segregation of the basal bodies and separation of the flagella throughout their entire length is observed (Fig. 5*B1*), in RNAi-induced cells, the two flagella are only partially separated (Fig. 5*B2*). These observations indicate that depletion of UMSBP affects cytokinesis as well as the minicircle replication and kDNA networks segregation.

Discussion

RNAi of *tb*UMSBP2, unlike *tb*UMSBP1, had deleterious effects on both cell morphology (Fig. *1F* 2 and 3) and cell growth (Fig. 1*B*). We interpreted the significant increase in nuclei size, observed in *tbUMSBP2* knocked-down cells (Fig. 1*F*2), as being the result of impaired nuclear mitosis in these cells. We hypothesize that nuclear DNA synthesis may have occurred normally in these cells; however, DNA segregation and the subsequent nuclear division were impeded. In accord with this notion was the generation of zoid cells in RNAi cells (Fig. 1*F*3), which probably resulted from the division of cells that have replicated their kDNA but were unable to go through nuclear mitosis, suggesting tbUMSBP2 involvement in this process. Its effect on the process of mitosis may be indirect, because our immunofluorescence analyses have detected only mitochondrial localization for UMSBP.

The absence of detectable effect of tbUMSBP1 RNAi could be explained by *tb*UMSBP2 functionally compensating for its loss. Indeed, analyses of *T. brucei* cells, in which both *tbUMSBP* genes were knocked down simultaneously, results in a series of phenotypic changes that add and modify the effects observed in cells in which only the *tbUMSBP2* gene was knocked down.

First, RNAi of both *tbUMSBP* genes resulted in a defined effect on the replication of kDNA minicircles (Fig. 3). These results suggest that depletion of the tbUMSBPs does not affect the prereplication release of covalently closed minicircles from the network but interferes with the initiation of their replication. Minicircle replication is not completely inhibited in these cells but continues, at a lower rate (≈50% compared with the uninduced control). It is possible that residual UMSBP in the knocked-down cells, was sufficient to support the observed rate of minicircle replication. Another possibility is that this process is not directed by the UMSBP-bound origin but by an alternative initiation site in the minicircle molecule. It is also possible that other origin-binding proteins, such as the *T. brucei* p38, which binds the minicircle replication origin (24), could partially substitute for the loss of UMSBP function.

Second, fluorescence microscopy has shown that, in addition to the large nuclei observed in cells undergoing RNAi for tbUMSBP2 (Fig. 1*F*2), simultaneous RNAi of both *tbUMSBPs* induced very large and intensely fluorescent kinetoplasts (Fig. 2*D*2). Analyses of DAPI-stained isolated networks as well as electron microscopy of thin sections of these cells (Fig. 4 *A* and *C*) suggest that the induced cells contain unsegregated kDNA networks. Furthermore, *in situ* labeling of the newly replicated gapped minicircle with fluorescent dUTP indicates that most of these large networks are still replicating (Fig. 5*A*) but unable to go through the kinetoplast segregation process. We suggest that the emergence of the giant kDNA networks is the result of minicircle replication that is not completely blocked in the RNAi cells (Fig. 3), along with impairment of kDNA segregation.

Third, after separation of the two basal bodies, in cells undergoing RNAi for both *tbUMSBP* genes, we often observed two basal bodies with linked flagella that are attached to a single large kinetoplast (Fig. 5*B*). It appears that these basal bodies and flagella have started their segregation but have been interrupted, resulting in cytokinesis block and cell-cycle arrest (Figs. 2*D* and 5*B*). In the case of several other kDNA replication proteins silenced by using RNAi (1, 25–27), it has been found that, although kDNA has not been properly replicated, it has nevertheless gone through a segregation process, which resulted in an uneven segregated networks, creating one cell with a minimal kDNA network and another with a very small nonfunctional kDNA (23). Such a process led to shrinkage of the network and eventually to kDNA loss. Unlike these proteins that function at the late stages of kDNA replication, UMSBP was implicated here with early events during minicircle replication. Remarkably, we could not detect shrunken kDNA networks, but instead, we observed here the generation of giant kDNA networks that do not segregate.

Previous publications have suggested that nuclear DNA replication or mitosis does not have to be completed in order for cytokinesis to occur (15, 28). Silencing of *UMSBP* results in cell-cycle arrest and impedes mitosis. One possible explanation for this effect could be that the inability of the kinetoplast DNA to replicate or segregate activates a cell-cycle checkpoint, which results in a cell-cycle block. In a recent report, the ablation of the single *DYNAMIN* gene in *T. brucei* by RNAi, resulted in the inhibition of the kDNA segregation and, as a consequence, in cell cycle arrest and a disturbance of the cytokinesis process (29). We suggest the existence of a checkpoint, which could be activated when either minicircle replication does not initiate properly or kinetoplast DNA segregation is compromised.

Unlike in most other eukaryotic cells, where mitochondrial DNA replication occurs throughout the entire cell cycle, trypanosomal kinetoplast S phase is tightly coordinated with nuclear S phase. We propose here that the interaction of UMSBP with the minicircle replication origin controls minicircle replication initiation. UMSBP may also play a role in coordinating kinetoplast and nuclear S phases. Hence, depletion of UMSBP has a direct effect on minicircle replication initiation, and this effect is communicated to the nucleus and has an indirect effect on nuclear S phase, as seen by the accumulation of cells with more than 4n DNA content. Thus, UMSBP may provide an essential checkpoint in the control of the trypanosomatid cell cycle.

Materials and Methods

Plasmid Constructs. For construction of RNAi vectors, PCR was used (for primers see SI Table 2) to amplify a 167-bp fragment of the gene Tb10.70.0800 (*tbUMSBP1*) and a 198-bp fragment of Tb10.70.0820 (*tbUMSBP2*) gene, which were ligated into pZJM (13) to yield pZJMBP1 and pZJMBP2, respectively. To construct the double gene-knockdown plasmid (pZJMBP1 and -2), the same fragment from Tb10.70.0820 (*tbUMSBP2*) was amplified, except that the forward primer also contained HindIII linkers and was then ligated into a pZJMBP1 construct digested with HindIII.

Trypanosomes Growth and Transfection. Procyclic *T. brucei* strain 29-13 (30), which harbors genes for T7 RNA polymerase and the tetracycline repressor, was grown and transfected as described (13, 26). Selection was applied in the presence of 2.5 μg/ml phleomycin, and the cells were grown for 2 weeks to form stable lines. Cell cultures were then cloned by limiting dilution. Induction of dsRNA performed, in a medium containing 1 μg/ml tetracycline.

Northern Blot Hybridization. Total RNA was purified by using TRI REAGENT preparation (Molecular Research Center). The ^{32}P-labeled probes were prepared by random priming of the PCR products used as inserts in the pZJM vector. Electrophoresis, blotting, and hybridization were as described (26).

Preparation of *T. brucei* Cleared Cell Extracts. Cells were harvested and resuspended (5×10^8 cells per milliliter) in Nonidet P-40 lysis buffer, containing 10 mM NaPi, pH 7.2, 1% Nonidet P-40,

2 mM EDTA, 0.5 M NaCl, 5 mM DTT, 1 mM PMSF, 5 μg/ml aprotinin, 1 μg/ml leupeptin, 3 mM benzamidine, and 1 μg/ml antipain. The cells were incubated on ice for 30 min and then centrifuged at 20,000 $\times$ *g* for 30 min at 4°C. For Western blot analyses, 20 μg of cleared cell extracts, drawn at 2-day intervals during the RNAi induction, were withdrawn. SDS/PAGE, Western blot and EMSA analyses were performed as described (10).

Immunofluorescence. UMSBP immunolocalization in *T. brucei* cells was performed as we have described (10), except that cells were fixed in 1% paraformaldehyde for 1 min, and Tween-20 was omitted from the blocking buffer. For the RNAi phenotype analysis, cells were fixed as described above, except that 4% paraformaldehyde in PBS was used for 5 min. For basal body and paraflagellar rod staining, cells were fixed in methanol at −20°C, overnight and then rehydrated with PBS. The slides were incubated with nondiluted BBA4 antibody and a 1:5 dilution of Mab25 antibodies directed against *T. brucei* exoneme protein (31) for 60 min and then for 45 min with a 1:150 dilution of FITC-conjugated goat anti-mouse (Jackson ImmunoResearch). BBA4 antibody was a generous gift of Keith Gull (University of Oxford, Oxford, U.K.). Isolated kDNA networks were allowed to settle on a 0.01% poly-L-lysine-coated slide for 30 min and were then stained with DAPI (2 μg/ml) for 2 min and washed twice with PBS for 5 min. Slides were examined by using a Zeiss Axioscope 2 imaging E microscope and images captured by a RETIGA EXi fast 1394 camera (Q imaging) using Image Pro Plus version 5.1.2 (Media Cybernetics). Measurements of the fluorescence intensity and the area occupied by kinetoplasts and nuclei were conducted by using Image pro plus version 5.1.2 (Media Cybernetics) and their statistic analyses performed by using One-way ANOVA program.

Whole-cell DNA and kDNA Purification and Analysis. To detect free minicircles, DNA was prepared, fractionated, and transferred to membranes as described in ref. 26, except that 300 ng of DNA was loaded in each well. kDNA networks were prepared as described (32). Cells (2×10^8) were harvested every 2 days after RNAi induction.

Electron Microscopy. Cells (4×10^8) of noninduced culture and 2×10^8 of RNAi induced cells (pZJMBP1 and -2, 144 h) were harvested by centrifugation at 1,000 $\times$ *g* for 15 min at room temperature and immediately fixed in 25 ml of 4% paraformaldehyde, 4% glutaraldehyde, and 0.2% tannic acid in 0.1 M cacodylate buffer, pH 7.0, at room temperature for 2 h. Samples were postfixed in osmium tetroxide, block stained in 2% uranyl acetate, dehydrated, and embedded in Spurr's resin (33). Sections were stained and visualized in a Philips CM10 electron microscope.

This paper is dedicated to the memory of Professor Arthur Kornberg, an esteemed biochemist, a wonderful mentor, and a friend. We thank Prof. Keith Gull for his generous gift of BBA4 antibodies and Gadi Shtepel and Efrat Dor for their help with the statistical analyses. This study was supported, in part, by United States–Israel Binational Science Foundation Grant 2005023 and by Israel Science Foundation Grant 54/06.

1. Liu B, Liu Y, Motyka SA, Agbo EE, Englund PT (2005) *Trends Parasitol* 21:363–369.
2. Shlomai J (2004) *Curr Mol Med* 4:623–647.
3. Woodward R, Gull K (1990) *J Cell Sci* 95:49–57.
4. Tzfati Y, Abeliovich H, Kapeller I, Shlomai J (1992) *Proc Natl Acad Sci USA* 89:6891–6895.
5. Abeliovich H, Tzfati Y, Shlomai J (1993) *Mol Cell Biol* 13:7766–7773.
6. Tzfati Y, Abeliovich H, Avrahami D, Shlomai J (1995) *J Biol Chem* 270:21339–21345.
7. Tzfati Y, Shlomai J (1998) *Mol Biochem Parasitol* 94:137–141.
8. Hertz-Fowler C, Peacock CS, Wood V, Aslett M, Kerhornou A, Mooney P, Tivey A, Berriman M, Hall N, Rutherford K, *et al.* (2004) *Nucleic Acids Res* 32:D339–D343.
9. Abu-Elneel K, Kapeller I, Shlomai J (1999) *J Biol Chem* 274:13419–13426.
10. Abu-Elneel K, Robinson DR, Drew ME, Englund PT, Shlomai J (2001) *J Cell Biol* 153:725–734.
11. Drew ME, Englund PT (2001) *J Cell Biol* 153:735–744.
12. Wirtz E, Leal S, Ochatt C, Cross GA (1999) *Mol Biochem Parasitol* 99:89–101.
13. Wang Z, Morris JC, Drew ME, Englund PT (2000) *J Biol Chem* 275:40174–40179.
14. Chen Y, Hung CH, Burderer T, Lee GS (2003) *Mol Biochem Parasitol* 126:275–279.
15. Ploubidou A, Robinson DR, Docherty RC, Ogbadoyi EO, Gull K (1999) *J Cell Sci* 112:4641–4650.
16. Guilbride DL, Englund PT (1998) *J Cell Sci* 111:675–679.
17. Saxowsky TT, Choudhary G, Klingbeil MM, Englund PT (2003) *J Biol Chem* 8:8.
18. Sinha KM, Hines JC, Downey N, Ray DS (2004) *Proc Natl Acad Sci USA* 101:4361–4366.
19. Sinha KM, Hines JC, Ray DS (2006) *Eukaryot Cell* 5:54–61.
20. Gull K (1999) *Annu Rev Microbiol* 53:629–655.
21. Robinson DR, Gull K (1991) *Nature* 352:731–733.
22. Woods A, Sherwin T, Sasse R, MacRae TH, Baines AJ, Gull K (1989) *J Cell Sci* 93(Pt 3):491–500.
23. Wang Z, Drew ME, Morris JC, Englund PT (2002) *EMBO J* 21:4998–5005.
24. Liu B, Molina H, Kalume D, Pandey A, Griffith JD, Englund PT (2006) *Mol Cell Biol* 26:5382–5393.
25. Klingbeil MM, Motyka SA, Englund PT (2002) *Mol Cell* 10:175–186.
26. Wang Z, Englund PT (2001) *EMBO J* 20:4674–4683.
27. Downey N, Hines JC, Sinha KM, Ray DS (2005) *Eukaryot Cell* 4:765–774.
28. Hammarton TC, Engstler M, Mottram JC (2004) *J Biol Chem* 279:24757–24764.
29. Chanez AL, Hehl AB, Engstler M, Schneider A (2006) *J Cell Sci* 119:2968–2974.
30. Wirtz E, Hoek M, Cross GA (1998) *Nucleic Acids Res* 26:4626–4634.
31. Pradel LC, Bonhivers M, Landrein N, Robinson DR (2006) *J Cell Sci* 119:1852–1863.
32. Perez-Morga D, Englund PT (1993) *J Cell Biol* 123:1069–1079.
33. Spurr AR (1969) *J Ultrastruct Res* 26:31–43.
34. Zick A, Onn I, Bezalel R, Margalit H, Shlomai J (2005) *Nucleic Acids Res* 33:4235–4242.
35. Johnson CE, Englund PT (1998) *J Cell Biol* 143:911–919.